Nuclear collective motion with full nonlinearity

Michel Baranger,[1] Michael Strayer,[2] and Jian-Shi Wu[3]
[1]*Center for Theoretical Physics and Laboratory for Nuclear Science, Massachusetts Institute of Technology, Cambridge, Massachusetts 02139-4307*
[2]*Physics Division, Oak Ridge National Laboratory, Oak Ridge, Tennessee 37831-6373*
[3]*Department of Natural Sciences, Fayetteville State University, Fayetteville, North Carolina 28301*
(Received 12 August 2002; published 28 January 2003)

The periodic solutions previously considered for nuclear time-dependent Hartree-Fock problems are recalculated by a new method which is more accurate and reliable. It starts from a first guess of the entire periodic trajectory, instead of a first guess of the initial state. An exact solution of the discretized nonlinear equations is then obtained in three to five iterations involving, once again, the entire trajectory. The resulting families of solutions, and in particular the relationship between the period and the energy, are much more complicated than previously thought. The meaning of this outcome is discussed.

DOI: 10.1103/PhysRevC.67.014318 PACS number(s): 21.60.Jz, 24.10.Cn, 24.30.Cz

I. INTRODUCTION

This is a report on the continuation of our calculations of nuclear collective motion with full inclusion of nonlinearity. In a first paper [1] we presented our early results for the monopole oscillations of ^{4}He based on a simple nuclear model of the Skyrme type. In our next paper [2] we discussed in detail the motivation for this kind of investigation, which involves a mean-field approximation with a classical aspect, a search for the periodic solutions of the dynamics of the mean field, and a requantization process. In the same paper we also gave the details of the discretization procedure and of the numerical method, as well as a set of new results for ^{16}O and more complete ones for ^{4}He. The present publication is devoted mostly to a new and very different algorithm for solving the same numerical problems and to the presentation of extensive results obtained with it for the collective monopole motion of ^{4}He. The emphasis is more technical than in the two previous papers, an attitude justified by the fact that this new method is more reliable, faster, and more accurate than the previous one. With it we hope to extend the calculations eventually to bigger nuclei and to nonspherically symmetric kinds of collective motion. We shall assume the reader to be familiar with the contents of Secs. III and IV of Ref. [2]; we shall not repeat this material here.

The superior accuracy of the new method has an interesting, and perhaps unexpected, consequence. The nonlinearity manifests itself by producing a large variety of resonances. The (E,τ) plot gets transformed from a simple smooth curve to a highly capricious collection of lines. See, for instance, Fig. 2, below. Most of the resonances are quite narrow, and they were invisible in the previous approach. Their origin is clear. In a many-dimensional linear system, consider two different types of periodic motion. They are uncoupled in general, but their periods vary with energy, and therefore there are discrete points in the (E,τ) plane where their two periods have a simple rational ratio. This is where the resonances will originate, because any amount of nonlinearity, even very small, will couple the two modes there. Actually, most of these resonances are very narrow, and they cannnot have an effect on the collective motion after quantization, because quantum mechanics has a way of smoothing out classical details over a phase space volume measured by a power of Planck's constant. A few of the resonances, however, appear to be wider and not so easy to dismiss. In the future, we want to use the present work to study the collective motion of nuclei heavier and more interesting than ^{4}He, and then these wider resonances could have a big impact on how we think about collective motion [3–5].

Previous calculations of cyclical time-dependent Hartree-Fock (TDHF) motion have made use of what is sometimes called ''the tail-chasing method'' [6,7]. One starts with some well-chosen Slater determinant, one evolves it one time step at a time with a good unitary kernel, and at some point one attempts to close the trajectory somehow, by using one of many possible *ad hoc* tricks [8]. These tricks usually involve large numbers of iterations, often thousands or even hundreds of thousands. The method that we introduce now is very different, because we consider the entire time evolution all at once. We start with a well-chosen guess, not for the initial state, but for the complete periodic trajectory, all times included. Then we proceed to refine this guess by successive iterations using the Newton-Raphson method. The remarkable fact is that very few iterations are necessary, three to five usually, and that this number of needed iterations is *independent of the size of the problem*. Of course there are other difficulties, as we shall see.

In the following, we first write down the equations to be solved (Sec. II). These equations include all times. Then we focus on the periodicity and we make sure that we have the same number of variables as equations (Sec. III). We bring in time-reversal invariance (Sec. IV). We examine in some detail the Newton-Raphson process and we discuss the numerical difficulties (Sec. V). We show how to generate the very first guess (Sec. VI). We show and discuss some results (Sec. VII). And finally we consider the future (Sec. VIII).

II. EQUATIONS OF MOTION

Since this paper considers only ^{4}He, there is only one single-particle wave function $\varphi(\mathbf{r},t)$, with a degeneracy of

$g=4$. Recall from Sec. IV of [2] that we discretize with a time index n and a time step ϵ. According to Eqs. (27) and (28) of [2], our equations of motion are

$$-\frac{2i}{\epsilon}(|\varphi_{n+1}\rangle-|\varphi_n\rangle)+H_{n+1/2}(|\varphi_{n+1}\rangle+|\varphi_n\rangle)=0. \quad (1)$$

After substitution from Eqs. (29) and (31) of [2], this is

$$-\frac{2i}{\epsilon}(|\varphi_{n+1}\rangle-|\varphi_n\rangle)+[K-\lambda-\alpha(\rho_{n+1}+\rho_n)+\beta(\rho_{n+1}^2+\rho_{n+1}\rho_n+\rho_n^2)](|\varphi_{n+1}\rangle+|\varphi_n\rangle)=0. \quad (2)$$

This takes care of the time dependence. Now we show the space dependence.

This is monopole motion; hence, there is no angular momentum. Equation (37) of [2] becomes

$$\varphi_n(\mathbf{r})=\frac{u_n(r)}{\sqrt{4\pi}\ r}. \quad (3)$$

This defines the usual radial wave function u, which behaves effectively like a one-dimensional wave function. It must vanish at $r=0$ and also at some arbitrary large radius $r=R$. It is usually complex, except for the ground state. We discretize r according to the end point method (see Sec. IV of [2]). We divide the interval $0\leqslant r\leqslant R$ into $M+1$ equal subintervals of size σ. For $1\leqslant m\leqslant M$ we define u_m as the value of $u(r)$ at one of the points separating two subintervals. In addition, it is useful to define $u_0=u_{M+1}=0$ to represent the fact that $U(r)$ must vanish at the ends of the interval. According to Eqs. (22) and (23) of [2], we represent the kinetic energy operator K by the matrix

$$k_{mm'}=\frac{1}{2\sigma^2}(2\delta_{mm'}-\delta_{m+1,m'}-\delta_{m-1,m'}) \quad \text{for} \quad 1\leqslant(m,m')\leqslant M. \quad (4)$$

This leads to the expressions

$$(Ku)_m=\sum_{m'} k_{mm'}u_{m'}=-\frac{1}{2\sigma^2}(u_{m+1}-2u_m+u_{m-1}), \quad (5)$$

$$(u^*,Ku)=\sigma\sum_{mm'} u_m^*k_{mm'}u_{m'}=\frac{1}{2\sigma}\sum_{m=0}^{M}|u_{m+1}-u_m|^2. \quad (6)$$

We can now introduce this space discretization into the equations of motion (2). All terms are diagonal in m except for K. The variables are u_{mn} and the equations are

$$-\frac{2i}{\epsilon}(u_{m,n+1}-u_{mn})+\sum_{m'} k_{mm'}(u_{m',n+1}+u_{m'n})+[-\lambda-\alpha(\rho_{m,n+1}+\rho_{mn})+\beta(\rho_{m,n+1}^2+\rho_{m,n+1}\rho_{mn}+\rho_{mn}^2)](u_{m,n+1}+u_{mn})=0. \quad (7)$$

The density ρ, Eq. (38) of [2], is given by

$$\rho_{mn}=\frac{g}{4\pi\sigma^2m^2}|u_{mn}|^2. \quad (8)$$

It will be necessary to have discretized expressions for the normalization P of u and the total many-body energy. We showed in [2] that these two quantities are exactly conserved by the numerical algorithm. As first pointed out in Ref. [9], the expression for P, which should be unity, is

$$P=\sigma\sum_{m=1}^{M}|u_{mn}|^2\equiv P_n. \quad (9)$$

The total many-body energy per particle (i.e., divided by g) is, according to Eq. (4) of [2]

$$E=E_{Kn}+E_{Vn}\equiv E_n, \quad (10)$$

with

$$E_{Kn}\equiv\sigma\sum_{mm'} u_{mn}^*k_{mm'}u_{m'n}\equiv\frac{1}{2\sigma}\sum_{m=0}^{M}|u_{m+1,n}-u_{mn}|^2 \quad (11)$$

$$E_{Vn}\equiv\sigma\sum_{m=1}^{M}(-\alpha\rho_{mn}+\beta\rho_{mn}^2)|u_{mn}|^2. \quad (12)$$

The value of λ is not determined yet. This will come in Sec. III.

In Sec. V we shall solve the equations of motion (7) by the Newton-Raphson method, which involves a linearization in the vicinity of a first guess. Because ρ, Eq. (8), contains the absolute value of u, the linearization turns out to be tricky if we use as variables the complex quantities u_{mn}. It is easier to separate u into its real and imaginary parts and to have nothing but real variables and equations. We do this,

$$u_{mn}=v_{mn}+iw_{mn} \quad (13)$$

(note that w is *not* the SP potential which occurs throughout Ref. [2]), and Eqs. (7) – (12) become the real part of the equations of motion,

$$2(w_{m,n+1}-w_{mn})/\epsilon+\sum_{m'} k_{mm'}(v_{m',n+1}+v_{m'n})+[-\lambda-\alpha(\rho_{m,n+1}+\rho_{mn})+\beta(\rho_{m,n+1}^2+\rho_{m,n+1}\rho_{mn}+\rho_{mn}^2)](v_{m,n+1}+v_{mn})=0; \quad (14)$$

the imaginary part of the equations of motion,

$$-2(v_{m,n+1}-v_{mn})/\epsilon+\sum_{m'} k_{mm'}(w_{m',n+1}+w_{m'n})+[-\lambda-\alpha(\rho_{m,n+1}+\rho_{mn})+\beta(\rho_{m,n+1}^2+\rho_{m,n+1}\rho_{mn}+\rho_{mn}^2)](w_{m,n+1}+w_{mn})=0; \quad (15)$$

the energy equations (one for each n, but E is actually independent of n)

$$E_n \equiv \frac{1}{2\sigma}\sum_{m=0}^{M}[(v_{m+1,n}-v_{mn})^2+(w_{m+1,n}-w_{mn})^2] + \sigma\sum_{m=1}^{M}(-\alpha\rho_{mn}+\beta\rho_{mn}^2)(v_{mn}^2+w_{mn}^2)=E; \quad (16)$$

and the probability equations, (same remark)

$$P_n \equiv \sigma\sum_{m=1}^{M}(v_{mn}^2+w_{mn}^2)=P=1, \quad (17)$$

with the definition

$$\rho_{mn}=\frac{g}{4\pi\sigma^2 m^2}(v_{mn}^2+w_{mn}^2). \quad (18)$$

III. CYCLES

We are now ready to look for the periodic solutions, which we call cycles. For a cycle the time index n goes only through N distinct values, which we usually choose as

$$n=0,1,2,\ldots,N-1, \quad (19)$$

and with the next time step the solution repeats itself:

$$v_{mN}=v_{m0}, \quad w_{mN}=w_{m0} \quad \text{for all } m. \quad (20)$$

The period of the cycle is

$$\tau=N\epsilon. \quad (21)$$

It is essential that the number of equations match the number of variables. The space index m takes M values. The time index n takes N values. This makes $2MN$ variables v_{mn}, w_{mn}. There are two more variables. One is the quasienergy λ. The other requires some discussion. In Sec. III of [2], we saw that cycles occur in one-parameter families, each family being represented in the (E,τ) plane by a line. We need to know what point on this line we wish to calculate. Thus, we must fix *a priori* either the value of E or the value of τ. The other quantity (the one we have not fixed) must come out of the calculation; this is our last variable. If we fix E, τ becomes a variable; if we fix τ, E becomes a variable. Actually, it turns out to be necessary, as we shall see, to do it sometimes one way and sometimes the other, though one should never mix both in the same calculation. Thus there are $2MN+2$ variables. Now we must count equations.

Each one of the equations (14) and (15) exists for $1\leqslant m \leqslant M$ and $0\leqslant n\leqslant N-1$. This should add up to $2MN$ equations. But it does not, since the equations are not independent. There are two relations between these $2MN$ equations, so that actually the number of independent equations in Eqs. (14) and (15) is $2MN-2$. The reasons for this are probability conservation and energy conservation. If we call R_{mn} the left-hand side of Eq. (14) and I_{mn} the left-hand side of Eq. (15), one of the relations between the $2MN$ equations is

$$\sum_{mn}[(w_{m,n+1}+w_{mn})R_{mn}-(v_{m,n+1}+v_{mn})I_{mn}]=0. \quad (22)$$

If we substitute the expressions for R_{mn} and I_{mn} into the left-hand side of Eq. (22), all the terms involving the kinetic energy, the quasienergy, and the interaction cancel out, and we are left with

$$\frac{2}{\epsilon\sigma}\sum_{n=0}^{N-1}(P_{n+1}-P_n), \quad (23)$$

where P_n is the normalization, or probability, per particle at time n, as defined in Eq. (17). Since we proved in [2] the identity $P_{n+1}\equiv P_n$, Eq. (23) vanishes identically. Thus Eq. (22) is a consequence of the conservation of probability. Similarly, the other relation between the $2MN$ equations is a consequence of the conservation of energy. It is

$$\sum_{mn}[(v_{m,n+1}-v_{mn})R_{mn}+(w_{m,n+1}-w_{mn})I_{mn}]=0. \quad (24)$$

Substituting R_{mn} and I_{mn} into the left-hand side again, we find that the terms multiplying $2/\epsilon$ cancel out, the kinetic energy terms give

$$\frac{1}{\sigma}\sum_{n}[(u_{n+1}^*,Ku_{n+1})-(u_n^*,Ku_n)], \quad (25)$$

the λ terms give

$$-\frac{\lambda}{\sigma}\sum_{n}(P_{n+1}-P_n), \quad (26)$$

and the interaction terms give

$$[-\alpha(\rho_{m,n+1}+\rho_{mn}) + \beta(\rho_{m,n+1}^2+\rho_{m,n+1}\rho_{mn}+\rho_{mn}^2)(|u_{m,n+1}|^2-|u_{mn}|^2), \quad (27)$$

which, given the simple relation (8) between ρ and $|u|^2$, is the same as

$$|u_{m,n+1}|^2(-\alpha\rho_{m,n+1}+\beta\rho_{m,n+1}^2)-|u_{mn}|^2(-\alpha\rho_{mn}+\beta\rho_{mn}^2). \quad (28)$$

Given the definition (16) of E_n, the left-hand side of Eq. (24) becomes

$$\frac{1}{\sigma}\sum_{n=0}^{N-1}[(E_{n+1}-\lambda P_{n+1})-(E_n-\lambda P_n)], \quad (29)$$

which vanishes if energy and probability are conserved. We have thus shown that the set of equations (13) and (14) amounts only to $2MN-2$ independent equations, but it is

not at all clear so far how one should proceed to get rid of two equations and make the set manifestly independent, which would be a good thing to do if we are to engage in numerical calculations. We return to this in a moment.

We saw that there are two special variables λ and (E or τ). How these should be determined is fairly obvious. One can think of λ as a Lagrange multiplier associated with the normalization condition, and it will be determined by the equation $P=1$, i.e., Eq. (17). There are N equations (17), but one is enough since all P_n are equal. For the other variable, let us assume for definiteness that we have fixed τ and we are looking for E: it will be determined by one of the N equations (16), or by the average of all N equations if one prefers.

Therefore, so far we have $2MN$ equations for the $2MN+2$ variables. Hence there must be two additional equations. These we call *antisliding* equations. The periodic solution that we are looking for is capable of sliding in two ways. There is phase sliding, which means that the solution $u(r,t)$ can be multiplied by an arbitrary constant phase factor $e^{i\chi}$. And there is time sliding, which means that the function $u(r,t+s)$, with arbitrary constant s, is just as good a solution as $u(r,t)$. Thus every solution of our problem is actually a doubly infinite set, with two arbitrary real parameters χ and s. The purpose of the two antisliding equations is to give definite values to χ and s. For the phase antisliding equation, we can say, for instance, that $u(r_0,t_0)$, at some point r_0 and presumably $t_0=0$, is real, i.e., $w(r_0,t_0)=0$. For a smoother prescription, we could say that the time average over one period of $w(r_0,t)$ should vanish. For the time antisliding equation, it works well to set to zero a particular Fourier component — for instance,

$$\sum_{n=0}^{N-1} \cos\frac{2\pi n}{N}|u_{m_0 n}|^2=0. \tag{30}$$

We now have as many equations as we have variables — namely, $2MN+2$. There are two antisliding equations, one probability equation, one energy equation, and $2MN-2$ dynamical equations to be picked somehow out of the $2MN$ equations (14) and (15). The question is, how do we pick them? Do we just throw away two equations chosen at random? That would be very dangerous. We did this at the beginning and we got some solutions, associated with the fact that Eqs. (22) and (24) can be satisfied sometimes even if a few of the quantities R_{mn} and I_{mn} do not vanish. What is needed is an answer to the problem which treats all equations on the same footing, preserving the symmetry between all values of m and n. We did find a very general answer of this sort eventually, but we are not going to present it here, because it turned out in the end that it was not needed. The situation simplified considerably when we took into account the one remaining symmetry of the model, time-reversal invariance. It took care of both the sliding problem and the dependent equations problem, as the next section shows.

IV. CONSEQUENCES OF TIME-REVERSAL INVARIANCE

For a scalar wave function such as our $u(r,t)$, time-reversal invariance makes the following statement. Given a solution $u^{(1)}(r,t)$ of the equation of motion, the function $u^{(2)}(r,t)$ defined by

$$u^{(2)}(r,t)\equiv u^{(1)*}(r,-t) \tag{31}$$

is also a solution. This is obvious from the continuous form of the equation of motion in [2]. We shall now prove the equivalent statement in discrete form — namely, that if we know a solution $u^{(1)}_{mn}\equiv v^{(1)}_{mn}+iw^{(1)}_{mn}$, then the quantity $u^{(2)}_{mn}\equiv v^{(1)}_{m,-n}-iw^{(1)}_{m,-n}$ is also a solution. To see this, start from Eqs. (14) and (15) for solution $u^{(1)}$ and change n into $-n-1$, which also changes $n+1$ into $-n$. This does nothing except relabel the time without changing its sense of flow; hence the equation is still true. Then replace $v^{(1)}_{m,-n-1}$, $v^{(1)}_{m,-n}$, $w^{(1)}_{m,-n-1}$, and $w^{(1)}_{m,-n}$ by $v^{(2)}_{m,n+1}$, $v^{(2)}_{mn}$, $-w^{(2)}_{m,n+1}$, and $-w^{(2)}_{mn}$, respectively. Note that $\rho^{(1)}_{m,-n-1}$ and $\rho^{(1)}_{m,-n}$ are replaced by $\rho^{(2)}_{m,n+1}$ and $\rho^{(2)}_{mn}$, respectively. Finally, verify that Eq. (14) has become the identical equation for $u^{(2)}_{mn}$, and similarly Eq. (15) has become the identical equation for $u^{(2)}_{mn}$ also, but with an overall change of sign.

There are now two possibilities: (1) $u^{(2)}$ and $u^{(1)}$ are one and the same solution, possibly after some time sliding and phase sliding; (2) $u^{(2)}$ and $u^{(1)}$ are different solutions. Both types of solutions exist. In classical dynamics with two degrees of freedom, these types of cycles are known, respectively, as *librations* (identical to each other except for possible time sliding) and *rotations* (not identical but occurring in pairs, each twin being the time reversed of the other). Here we shall look only at the simplest case, type 1. All random phase approximation (RPA) solutions are of this type. In the present paper, we shall start from an RPA solution and extend it into the nonlinear domain. This is a continuous evolution, which can never break the original time-reversal symmetry. Nonsymmetrical solutions, i.e., solutions of type 2, do exist, and they can be found as bifurcations of the time-symmetric ones, but we shall not look for them in the present paper.

Returning now to Eq. (31), suppose that there exists a solution $u^{(1)}(r,t)$ of type 1. This means that $u^{(2)}(r,t)$ is identical to it except for time sliding and phase sliding. Therefore it can be written

$$u^{(2)}(r,t)\equiv u^{(1)*}(r,-t)\equiv e^{i\chi}u^{(1)}(r,t+s), \tag{32}$$

χ and s being real constants. Now define

$$u^{(3)}(r,t)\equiv e^{i\chi/2}u^{(1)}\left(r,t+\frac{s}{2}\right) \tag{33}$$

and calculate $u^{(3)*}(r,-t)$, first by substituting in Eq. (33),

$$u^{(3)*}(r,-t)=e^{-i\chi/2}u^{(1)*}\left(r,-t+\frac{s}{2}\right), \tag{34}$$

and then by using the second equation (32) for $u^{(1)*}$,

$$u^{(3)*}(r,-t)=e^{-i\chi/2}e^{i\chi}u^{(1)}\left(r,t-\frac{s}{2}+s\right)\equiv u^{(3)}(r,t). \tag{35}$$

Thus we have found a solution $u^{(3)}(r,t)\equiv v^{(3)}(r,t)+iw^{(3)}(r,t)$ which remains identical to itself under time reversal, without extra sliding. This means that $v^{(3)}(r,t)$ is an even function of t and $w^{(3)}(r,t)$ is an odd function of t. We have just shown that every solution of type 1 can be written in the $u^{(3)}$ form. This is the form that we shall adopt for our cycle calculations. If the solution is a cycle, then v is also even with respect to $t=\tau/2$ and w is also odd, which means that w vanishes for both $t=0$ and $t=\tau/2$. It is clear that this choice eliminates all sliding possibilities, both in time and in phase. The time $t=0$ plays a very special role, and the phase at $t=0$ is 0.

In the discrete representation we now have

$$v_{m,-n}=v_{mn}, \quad w_{m,-n}=-w_{mn},$$

$$w_{m0}=0, \quad w_{m,N/2}=0. \tag{36}$$

The last equation supposes that we have chosen N even, which we always will. Let us count variables. In v_{mn} the ranges of m and n are

$$1\leqslant m\leqslant M, \quad 0\leqslant n\leqslant N/2, \tag{37}$$

which makes $M(N/2+1)$ variables. In w_{mn} the ranges are

$$1\leqslant m\leqslant M, \quad 0<n<N/2, \tag{38}$$

which makes $M(N/2-1)$ variables. The sum is MN. Add to this λ and either E or τ: the total number of variables is $MN+2$. Now let us count equations. We have Eq. (14) for the ranges

$$1\leqslant m\leqslant M, \quad 0\leqslant n\leqslant N/2-1, \tag{39}$$

which adds up to $MN/2$ equations, and Eq. (15) for the same ranges, giving another set of $MN/2$ equations. We have two more equations, one associated with probability and one with energy. We actually have N probability equations in Eq. (17) and N energy equations in Eq. (16), but we only need one of each type, since we already know that probability and energy are exactly conserved by the equations of motion. The best choice in each case is to take the average of all the equations. Hence we use as probability equation

$$\frac{1}{N}\left[2\sum_{n=1}^{N/2-1}P_n+P_0+P_{N/2}\right]=1, \tag{40}$$

where P_n is defined by the identity on the left-hand side of Eq. (17). Similarly we use as energy equation

$$\frac{1}{N}\left[2\sum_{n=1}^{N/2-1}E_n+E_0+E_{N/2}\right]=E, \tag{41}$$

where E_n is defined in Eq. (16). Recall that E can be either a variable or a constant. The same equation is used in both cases.

These are the $MN+2$ equations that are solved in the following section. It is good to realize that the argument of Sec. III, showing that Eqs. (14) and (15) are not independent, does not carry through any more, since we do not use all of these equations but only half of them. When the argument gets to Eq. (23), what we have instead is

$$\frac{2}{\epsilon\sigma}\sum_{n=0}^{N/2-1}(P_{n+1}-P_n), \tag{42}$$

which, by virtue of the identity $P_{n+1}\equiv P_n$, becomes

$$\frac{2}{\epsilon\sigma}(P_{N/2}-P_0). \tag{43}$$

$P_{N/2}$ and P_0 are not identical; hence there is no automatic vanishing here. Similar reasoning applies to Eq. (29). In other words, we do have $MN+2$ independent equations for $MN+2$ variables.

V. NUMERICAL SEARCH FOR CYCLES

A. Overview

We have found a large number (of the order of 1000) of solutions of the above equations. Each solution is a cycle with a certain period τ and a certain energy E. Plots of the relationship between E and τ [the (E,τ) plot] will be shown in Sec. VII. It is perfectly possible to have two different solutions with the same E and the same τ, but this is unusual since the solutions arrange themselves into continuous one-parameter families or lines in the (E,τ) plane, and crossings are rare. Each one of these cycles is obtained through the following steps:

(1) An educated guess is made for the cycle.

(2) The equations are linearized in the vicinity of the guess.

(3) The linear equations are solved, which yields a better guess.

(4) The process is repeated until convergence is achieved to double precision.

These are the steps which constitute the Newton-Raphson method. In a typical case, convergence is achieved with three to five iterations. The number of necessary iterations is approximately independent of the dimensionality of the problem; this is one of the advantages of using Newton-Raphson for large problems. In our work, each iteration took a few seconds on a very ordinary, vintage 1997, desktop computer.

As we mentioned in the Introduction, the main difference between the present method and other ways of finding time-dependent Hartree-Fock cycles, including our own work [1,2], is that here we always consider the complete periodic

trajectory all at once, instead of choosing a wave function at an initial time and then evolving it time step by time step. Consequently the present algorithm needs to handle simultaneously a much larger number of variables. This added difficulty is compensated by the fact that the resulting procedure is much more robust and stable. The present method is essentially the same as the ''monodromy method'' described and applied in [10]. The monodromy method is just one particular way of solving the same Newton-Raphson equations. Here we solve them by ''brute force'' instead. This is because the dimensionality of the present problem is much higher than in [10], which leads to a larger and more complicated monodromy matrix, which would necessitate much more programming, which would lead to an increased danger of error.

B. The guess

Since we know that the cycles lie on various continuous lines in the (E,τ) plane, we look for these lines, and we progress along each one of them in a continuous fashion: we use each found solution as the first guess for our next point in the family. This is the approach already used long ago in the first work of this type [10]. Here the difference between a large problem (like this one) and a small problem (like those of [10]) is not in the number of iterations necessary to achieve convergence, which is always three to five; it is in the fact that, for the large problem, you have to pick the next point much closer to the original one. In both cases, large and small, it is possible, and in fact rather common, to be overambitious in choosing the size of the (E,τ) jump and to find that the new Newton-Raphson solution converges to a cycle which looks very different from the family one has been following and is not connected continuously to it — a pleasant surprise, usually. It is also possible, and even more common, to find that Newton-Raphson does not converge at all — less pleasant, but not really surprising.

In this fashion, one can follow each continuous line as far as one wants. But how does one find that family in the first place? It is important to realize that families of cycles do not start or stop in the middle of nowhere: either they start at zero excitation energy — i.e., the ground state — or they form (E,τ) curves without loose ends, except possibly at infinity. They also bifurcate. Bifurcations were studied extensively in [10], but we have not done any systematic work on them for the present problem. We started our search for cycles by looking at energies very close to the ground state, where our equations become identical with those of the random phase approximation. We solved the RPA equations, which provided the starting points of the (E,τ) lines at low energy. All other cycles were found, either by the continuity process described earlier or by the jumping process described earlier. The details of the RPA solution are given in Sec. VI.

C. Linearized equations

Generally, suppose that one needs to solve the following p nonlinear equations in p variables x_i $(i=1,\ldots,p)$ or simply x,

$$f_j(x)=A_j, \quad j=1,\ldots,p, \tag{44}$$

where A_j is a constant, possibly 0. In the Newton-Raphson method, one starts with a guess, which we call x^0. Then one looks for a better answer, which we call $x^0+\delta x$, by linearizing the equations in the vicinity of x^0. We write this linearization in the form

$$\sum_{i=1}^{p} \frac{\partial f_j}{\partial x_i}(x^0)\,\delta x_i = R_j, \tag{45}$$

with

$$R_j \equiv A_j - f_j(x^0). \tag{46}$$

These are linear equations for the variables δx, in which our guess x^0 functions as a set of constants. Once the equations have been solved, the new guess becomes $x^0+\delta x$ and the process is repeated if necessary.

We now write the linearized form of the equations of motion (14) and (15) in a similar notation. Some manipulation needs to take place, and we find

$$\begin{aligned}
&\frac{2}{\epsilon}(\delta w_{m,n+1}-\delta w_{mn})+\frac{1}{2\sigma^2}(2\,\delta v_{m,n+1}+2\,\delta v_{mn}-\delta v_{m-1,n+1}-\delta v_{m-1,n}-\delta v_{m+1,n+1}-\delta v_{m+1,n})\\
&\quad-(\delta v_{m,n+1}+\delta v_{mn})[\alpha(\rho_{m,n+1}+\rho_{mn})-\beta(\rho_{m,n+1}^2+\rho_{m,n+1}\rho_{mn}+\rho_{mn}^2)+\lambda]\\
&\quad-\frac{g}{2\pi\sigma^2 m^2}(v_{m,n+1}+v_{mn})(\alpha-2\beta\rho_{m,n+1}-\beta\rho_{mn})(v_{m,n+1}\delta v_{m,n+1}+w_{m,n+1}\delta w_{m,n+1})\\
&\quad-\frac{g}{2\pi\sigma^2 m^2}(v_{m,n+1}+v_{mn})(\alpha-2\beta\rho_{mn}-\beta\rho_{m,n+1})(v_{mn}\delta v_{mn}+w_{mn}\delta w_{mn})\\
&\quad-(v_{m,n+1}+v_{mn})\,\delta\lambda+2(w_{m,n+1}-w_{mn})\,\delta\left(\frac{1}{\epsilon}\right)=R_{mn}^r,
\end{aligned} \tag{47}$$

$$
\begin{aligned}
&-\frac{2}{\epsilon}(\delta v_{m,n+1}-\delta v_{mn})+\frac{1}{2\sigma^2}(2\,\delta w_{m,n+1}+2\,\delta w_{mn}-\delta w_{m-1,n+1}-\delta w_{m-1,n}-\delta w_{m+1,n+1}-\delta w_{m+1,n})\\
&\quad-(\delta w_{m,n+1}+\delta w_{mn})[\alpha(\rho_{m,n+1}+\rho_{mn})-\beta(\rho_{m,n+1}^2+\rho_{m,n+1}\rho_{mn}+\rho_{mn}^2)+\lambda]\\
&\quad-\frac{g}{2\pi\sigma^2 m^2}(w_{m,n+1}+w_{mn})(\alpha-2\beta\rho_{m,n+1}-\beta\rho_{mn})(v_{m,n+1}\delta v_{m,n+1}+w_{m,n+1}\delta w_{m,n+1})\\
&\quad-\frac{g}{2\pi\sigma^2 m^2}(w_{m,n+1}+w_{mn})(\alpha-2\beta\rho_{mn}-\beta\rho_{m,n+1})(v_{mn}\delta v_{mn}+w_{mn}\delta w_{mn})\\
&\quad-(w_{m,n+1}+w_{mn})\delta\lambda-2(v_{m,n+1}-v_{mn})\delta\left(\frac{1}{\epsilon}\right)=R_{mn}^{i},
\end{aligned}
\tag{48}
$$

where R_{mn}^{r} and R_{mn}^{i} are the left-hand sides of Eqs. (14) and (15), respectively. The ranges of variation of m and n were given in Eqs. (39). One must also remember that v and w vanish for $m=0$ and $m=M+1$, and that w vanishes for $N=0$ and $n=N/2$. Note that the equations contain $\delta(1/\epsilon)$ since ϵ, or $\tau=N\epsilon$, is one of the possible variables (one variable must be either τ or E). Note also the presence of $\delta\lambda$, again one of the variables.

The linearized form of the probability equation (40) is

$$
\frac{2\sigma}{N}\sum_{m=1}^{M}\left[2\sum_{n=1}^{N/2-1}(v_{mn}\delta v_{mn}+w_{mn}\delta w_{mn})+v_{m0}\delta v_{m0}+v_{m,N/2}\delta v_{m,N/2}\right]=R^{p},
\tag{49}
$$

with

$$
R^{p}=1-\frac{1}{N}\left[2\sum_{n=1}^{N/2-1}P_n+P_0+P_{N/2}\right].
\tag{50}
$$

Finally, the linearized form of the energy equation (41) is

$$
\begin{aligned}
&\frac{1}{N}\sum_{m=1}^{M}\left[2\sum_{n=1}^{N/2-1}\left\{\frac{1}{\sigma}(2v_{mn}-v_{m-1,n}-v_{m+1,n})+2\sigma(-2\alpha\rho_{mn}+3\beta\rho_{mn}^2)v_{mn}\right\}\delta v_{mn}\right.\\
&\quad+2\sum_{n=1}^{N/2-1}\left\{\frac{1}{\sigma}(2w_{mn}-w_{m-1,n}-w_{m+1,n})+2\sigma(-2\alpha\rho_{mn}+3\beta\rho_{mn}^2)w_{mn}\right\}\delta w_{mn}\\
&\quad+\left\{\frac{1}{\sigma}(2v_{m0}-v_{m-1,0}-v_{m+1,0})+2\sigma(-2\alpha\rho_{m0}+3\beta\rho_{m0}^2)v_{m0}\right\}\delta v_{m0}\\
&\quad\left.+\left\{\frac{1}{\sigma}(2v_{m,N/2}-v_{m-1,N/2}-v_{m+1,N/2})+2\sigma(-2\alpha\rho_{m,N/2}+3\beta\rho_{m,N/2}^2)v_{m,N/2}\right\}\delta v_{m,N/2}\right]-\delta E=R^{e},
\end{aligned}
\tag{51}
$$

with

$$
R^{e}=E-\frac{1}{N}\left[2\sum_{n=1}^{N/2-1}E_n+E_0+E_{N/2}\right].
\tag{52}
$$

Here we have δE as a possible variable. We discuss in the next subsection when to choose E and when to choose τ as the variable. In practice, the program contains a binary parameter with the possible values "E fixed" and "τ fixed," and the same program solves both cases, depending on how this parameter has been set.

D. Solution

We define a precision V, which is simply the sum of the squares of the right-hand sides of the linearized equations

$$
\mathrm{V}=\sum_{m=1}^{M}\sum_{n=0}^{N/2-1}[(R_{mn}^{r})^2+(R_{mn}^{i})^2]+(R^{p})^2+(R^{e})^2.
\tag{53}
$$

Some care must be taken to ensure that, in a typical run, all the additive terms in V are very roughly of the same order of magnitude. If they are not, some multiplicative constants should be introduced. We keep performing Newton-Raphson

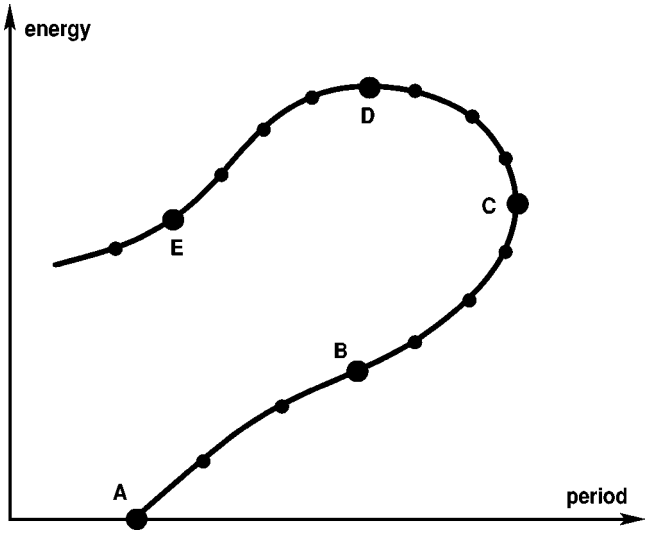

FIG. 1. Navigating an (E,τ) line. See text.

iterations until V has decreased sufficiently to jump around randomly due to the limited precision of the computer. For the machine we were using, given that most of the quantities in the equations were of order unity and given that we used mainly $M=15$ and $N=64$, this limit V turned out to be approximately 10^{-33}. Thus, our results are very accurate solutions of the given equations. This is an important remark, since our results might be considered strange in some quarters. We repeat that the number of iterations necessary to reach that level of precision was only three to five. We show the results in Sec. VII.

We solve the $MN+2$ $(=962$ in our case) linear equations with an all-purpose subroutine for real equations. There are several ways to speed up the calculation by using the fact that the matrix of the coefficients is fairly sparse, but we have not tried this so far; we just use a general method. Certainly, when we start calculating more complicated nuclei, we will need to pay attention to this point.

Even with a good algorithm and a modern computer, the process of following the families in the (E,τ) plane can be slow and tedious. It is very tempting to try to free oneself by automating it. So far, everyone who has tried to do this has failed. The apparent reason is that the landscape is chaotic and many unforeseeable accidents can happen. Each accident results in a diverging sequence of iterations and the absence of a suitable guess to continue the search. All the results presented in Sec. VII were obtained with somebody sitting at the computer and directing every step — a personal adventure akin to the exploration of a new continent. In the future, whoever succeeds in automating the process will have to allow for the following, at least: (1) places where the (E,τ) curve turns unexpectedly, and it becomes necessary to switch beween fixed τ and fixed E; (2) places where another curve approaches very closely and the convergence gets derailed unless extremely small steps are used; (3) the onset of a resonance, many examples of which can be seen in Sec. VII; (4) bifurcations, where it is possible for the program to get confused by the presence of several possibilities and to diverge as a result.

Finally, we shall explain why we need to have the choice between fixing τ and fixing E and then use the other quantity as one of the variables. The continuous families of cycles may follow any smooth curve in the (E,τ) plane. There is no theorem which says that there has to be a one-to-one correspondence between the values of E and the values of τ. A very common situation is the one shown in Fig. 1, where the curve possesses both a vertical tangent and a horizontal tangent. Suppose that we got our first cycle at point A by using the RPA. Then we proceed by small steps up the curve toward point B, then past point B. When we approach the vicinity of C, we need to pinpoint the next cycle to be calculated by giving its E. We cannot give its τ, because τ varies too slowly in the vicinity of C; if we try to give τ, we have a good chance of giving a τ that is completely wrong, and the program will refuse to converge. Hence we explore the vicinity of C by fixing E ahead of time and letting the program decide the value of τ; i.e., we treat τ as a variable. But after we have passed C and we arrive in the vicinity of D, the situation is reversed. Now we must fix τ ahead of time and let the program decide the value of E. Thus, somewhere between C and D, we must switch from fixed E to fixed τ. On the other hand, in any section of the curve which is not either nearly horizontal or nearly vertical, such as around point B or E, both fixed E and fixed τ will work and give identical results. The times necessary to do a fixed E calculation and a fixed τ calculation turn out to be the same.

VI. RANDOM PHASE APPROXIMATION

It is well known that the RPA can be obtained by linearizing the TDHF equations in the vicinity of the static HF ground state. We shall use this fact to generate the starting points of the (E,τ) families of cycles.

The TDHF equations of motion are Eqs. (14) and (15). We already linearized them in Eqs. (47) and (48). In these latter equations, we must now choose ''the guess'' to be the HF ground state. The latter has a real, time-independent wave function which we call u_{Gm}. The equation satisfied by u_{Gm} can be obtained from Eq. (14) by assuming no time dependence. It is

$$\sum_{m'} k_{mm'}u_{Gm'}+(-2\alpha\rho_{Gm}+3\beta\rho_{Gm}^2-\lambda_G)u_{Gm}=0, \tag{54}$$

where ρ_{Gm} is the density in the ground state and λ_G is the HF single-particle energy. This equation can be solved easily by a Newton-Raphson method. We now write Eq. (47) replacing v_{mn} by u_{Gm}, w_{mn} by 0, ρ_{mn} by ρ_{Gm}, λ by λ_G, and R^r_{mn} by 0 and using Eq. (8) for the ground state. We find (after division by 2)

$$\begin{aligned}(\delta w_{m,n+1}-\delta w_{mn})/\epsilon+\sum_{m'} k_{mm'}(\delta v_{m',n+1}+\delta v_{m'n})/2\\ +(-6\alpha\rho_{Gm}+15\beta\rho_{Gm}^2-\lambda_G)(\delta v_{m,n+1}+\delta v_{mn})/2\\ -u_{Gm}\delta\lambda=0.\end{aligned} \tag{55}$$

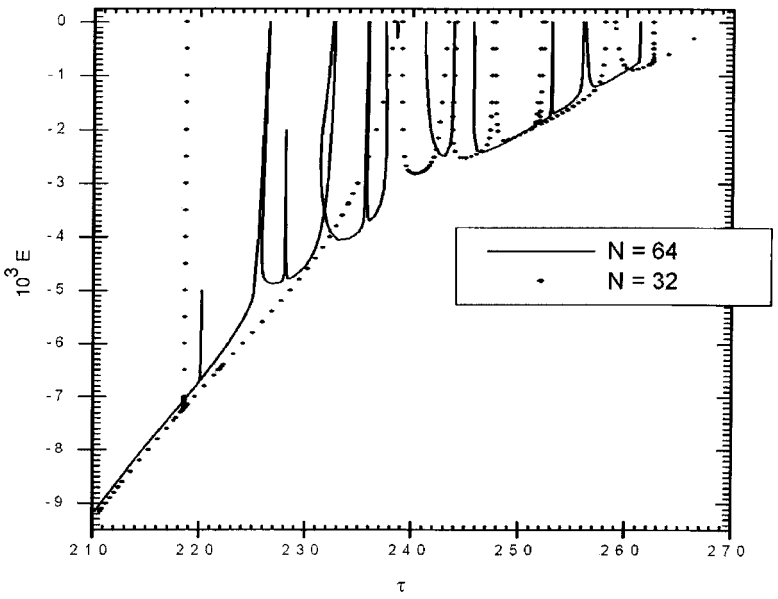

FIG. 2. Solid line: the breathing mode (E,τ) plot for $N=64$. Isolated points: same for $N=32$. The units are given at the beginning of Sec. VII.

We do the same for Eq. (48):

$$-(\delta v_{m,n+1}-\delta v_{mn})/\epsilon+\sum_{m'} k_{mm'}(\delta w_{m',n+1}+\delta w_{m'n})/2 +(-2\alpha\rho_{Gm}+3\beta\rho_{Gm}^2-\lambda_G)(\delta w_{m,n+1}+\delta w_{mn})/2=0. \tag{56}$$

In these equations, δv_{mn} and δw_{mn} are the small time-dependent increments that must be added to u_{Gm} to produce a harmonically oscillating solution. The equations are linear and homogeneous; therefore they have no nontrivial solution unless some special condition is met — namely, $1/\epsilon$ must be an eigenvalue of the matrix. As for $\delta\lambda$, it is not coupled to any other variable; therefore it can be taken to vanish.

To proceed further, we note that all the coefficients are time independent. Just as in linear differential equations with constant coefficients, this means that the functional form of the solution is harmonic. A convenient form which possesses the required symmetries is

$$\delta v_{mn}=A_m\cos\frac{2\pi n}{N},\quad \delta w_{mn}=B_m\sin\frac{2\pi n}{N}. \tag{57}$$

Using some simple trigonometric identities, we can write

$$(\delta v_{m,n+1}+\delta v_{mn})/2=A_m\cos\frac{\pi}{N}\cos\frac{2\pi(n+1/2)}{N},$$

$$(\delta v_{m,n+1}-\delta v_{mn})/2=-A_m\sin\frac{\pi}{N}\sin\frac{2\pi(n+1/2)}{N},$$

$$(\delta w_{m,n+1}+\delta w_{mn})/2=B_m\cos\frac{\pi}{N}\sin\frac{2\pi(n+1/2)}{N},$$

$$(\delta w_{m,n+1}-\delta w_{mn})/2=B_m\sin\frac{\pi}{N}\cos\frac{2\pi(n+1/2)}{N}. \tag{58}$$

Upon substitution into Eqs. (55) and (56), all time dependence disappears and we are left with

$$\frac{2}{\epsilon}\tan\frac{\pi}{N}B_m+\sum_{m'} k_{mm'}A_{m'}+(-6\alpha\rho_{Gm}+15\beta\rho_{Gm}^2-\lambda_G)A_m=0,$$

$$\frac{2}{\epsilon}\tan\frac{\pi}{N}A_m+\sum_{m'} k_{mm'}B_{m'}+(-2\alpha\rho_{Gm}+6\beta\rho_{Gm}^2-\lambda_G)B_m=0, \tag{59}$$

which are eigenvalue equations determining $(2/\epsilon)\tan(\pi/N)$, the eigenvalue, and A_m, B_m, the eigenvector. In the limit of large N, $(2/\epsilon)\tan(\pi/N)$ becomes $2\pi/N\epsilon\equiv\omega$, the angular frequency, and the equations become the traditional RPA equations for this problem.

In practice, we solve these equations, and we pick the eigenvalue that we want to work with, usually the most collective. We multiply the eigenvector by a coefficient small enough that, after adding u_{Gm} to δv_{mn}, the energy of the new guess will still be very close to that of the ground state. We also renormalize the guess to make its time-averaged probability equal to unity. Then we feed it to the main program. The latter works well in the vicinity of the ground state provided (1) the quantity which we hold fixed is E, not τ (otherwise the iterations lead back to the ground state) and (2) very small steps are taken. The size of the steps can be increased later.

VII. RESULTS

All the calculations presented here were done with $M=15$ radial points spaced by $\sigma=2$. Our units are such that $m=\hbar=c=1$. The energy unit is 939 MeV, the length unit is 0.2101 fm, and the time unit is 0.2101 fm/c. The parameters used for the interaction are $\alpha=46.905$, $\beta=13\ 360.33$.

The solid line in Fig. 2 is the (E,τ) plot — i.e., energy in

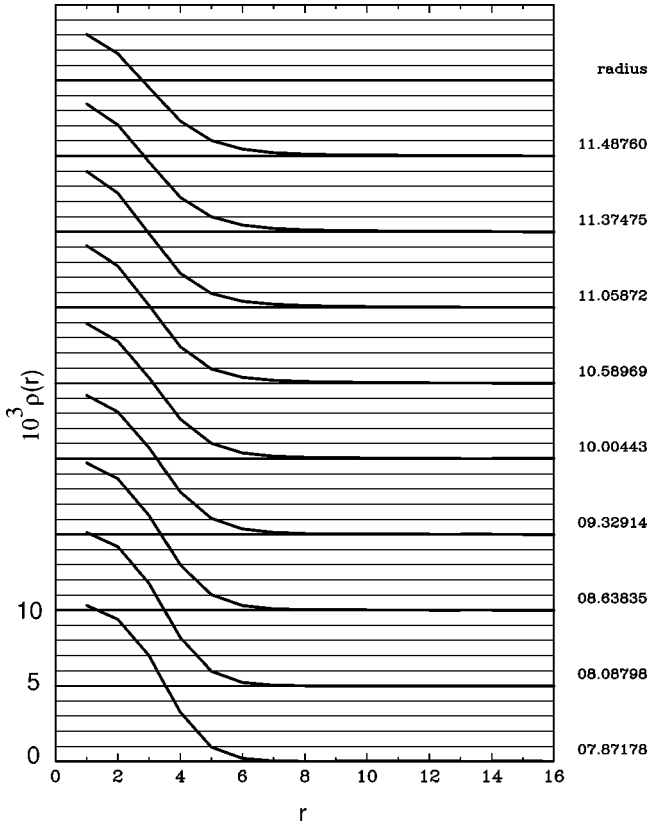

FIG. 3. This and all remaining figures plot the density $\rho(r,t)$ over a time interval of half a period. The abscissa is r in units of σ. The ordinate is ρ times 10^3 in units specified at the beginning of Sec. VII. The nine curves correspond to nine times separated by $\tau/16$. The curves have been displaced vertically by multiples of 5 (times 10^3) to make them clear. The rms radii at each time are given on the right. The top and bottom curves are at the special times of time-reversal symmetry — i.e., $n=0$ and $n=N/2$ in Sec. IV. The other half-period would be identical to this, but in reverse order. This cycle has $N=64$, $E=-6.4\times10^{-3}$, and $\tau=221.249$. It is on the main breathing line.

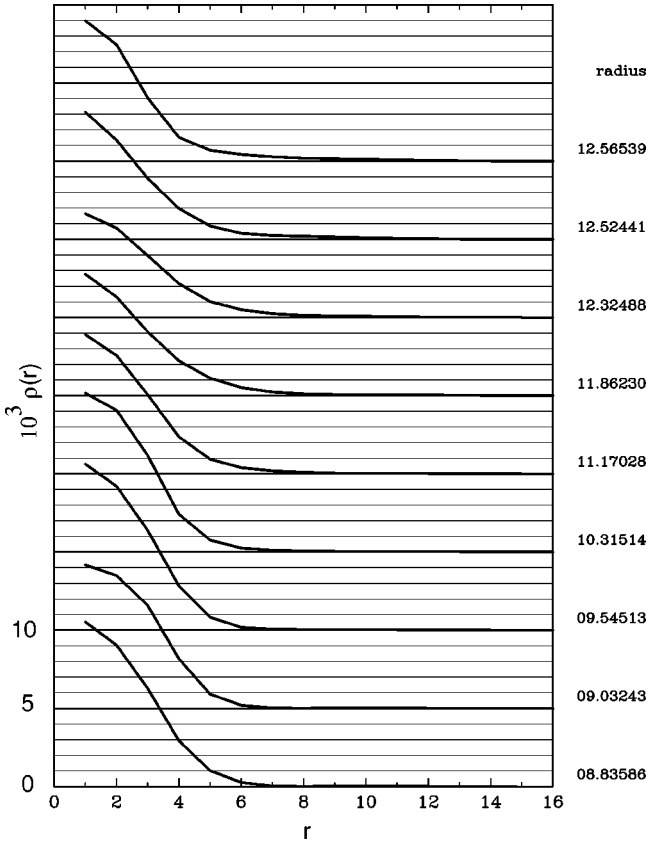

FIG. 4. Cycle on the main breathing line, $N=64$, $E=-3.983\ 53\times10^{-3}$, and $\tau=234.5$.

terms of period — for 64 time points ($N=64$). The ''resonances'' that we mentioned in the Introduction are in full view. The naive expectation of a smooth, gradual relationship could not be farther from the truth. The smooth curve imagined by our intuition is actually the bottom envelope, as we shall see.

Now we can understand why, in our previous calculations [1,2] and in those of other authors as well, there were regions of the (E,τ) plane where the iteration procedure could not be made to converge. This was very puzzling at the time, but now we can check that these regions were precisely those where resonances were happening, strongly perturbing the evolution of our wave function in a way that we did not comprehend. The beauty of the present method is that one always gets strong convergence, as long as the initial guess is close enough.

An obvious question arises. How much of this resonant behavior is due to the finiteness of the time mesh, and how much is independent of it? One way to begin answering is to compare two sets of results with different sets. So far we have only calculated with $N=16$, 32, and 64. Figure 2 also shows the $N=32$ results, as isolated points. The comparison between the two sets leads to the following tentative conclusions. First, the bottom envelope is roughly the same for both N's. It is also roughly the same as the smooth curve that we found previously [2], when we did less accurate calculations. As we shall see shortly, cycles close to this ideal smooth line do exhibit the ''breathing'' type of motion which the simple models imagine. Other cycles do not. Hence it is reasonably safe to conclude that the bottom envelope is the actual (E,τ) curve for the breathing mode.

The second conclusion is that most of the ''resonances'' do not seem to be the same for $N=32$ and $N=64$. Actually, the number of resonances is larger for $N=64$ than for $N=32$, and it was also larger for $N=32$ than for $N=16$. This number is expected to go on increasing with N, and the limit of $N\rightarrow\infty$ is not expected to be simple and smooth. Coming back to whether the resonances agree for the two N's, one should note that the widest resonance for $N=64$ overlaps with the widest resonance for $N=32$ and that the next two widest in each case almost overlap. These facts point to the following. For each value of N there are ''real'' resonances — i.e., resonances which remain as N gets large — and ''false'' resonances — i.e., resonances due to the finiteness of the time mesh and which change drastically when N changes. Both kinds increase in numbers as N increases. Both kinds have the same cause — namely, a simple ratio between the period of this breathing mode and the lower period of some

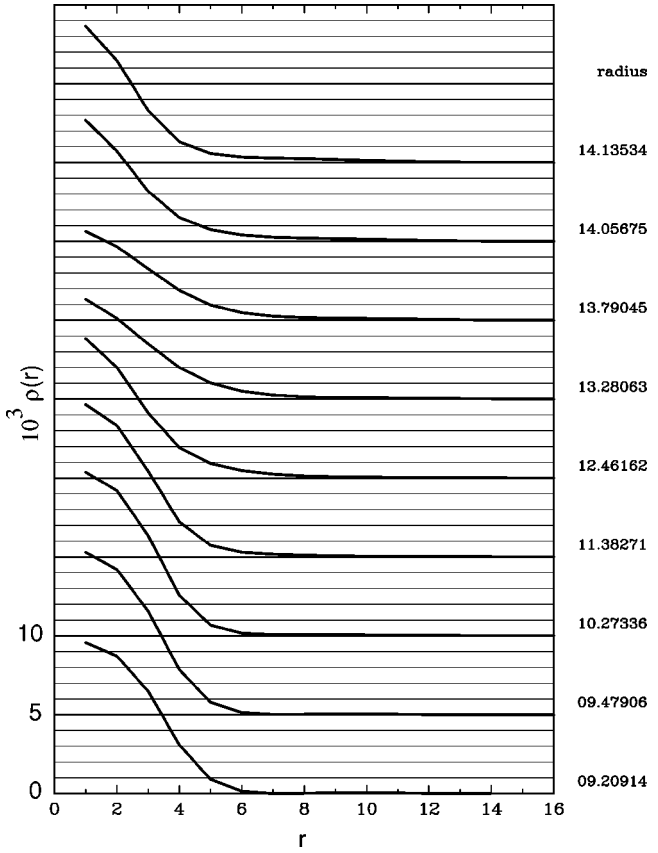

FIG. 5. Cycle on the main breathing line, $N=64$, $E=-1.959\ 81\times10^{-3}$, and $\tau=251$.

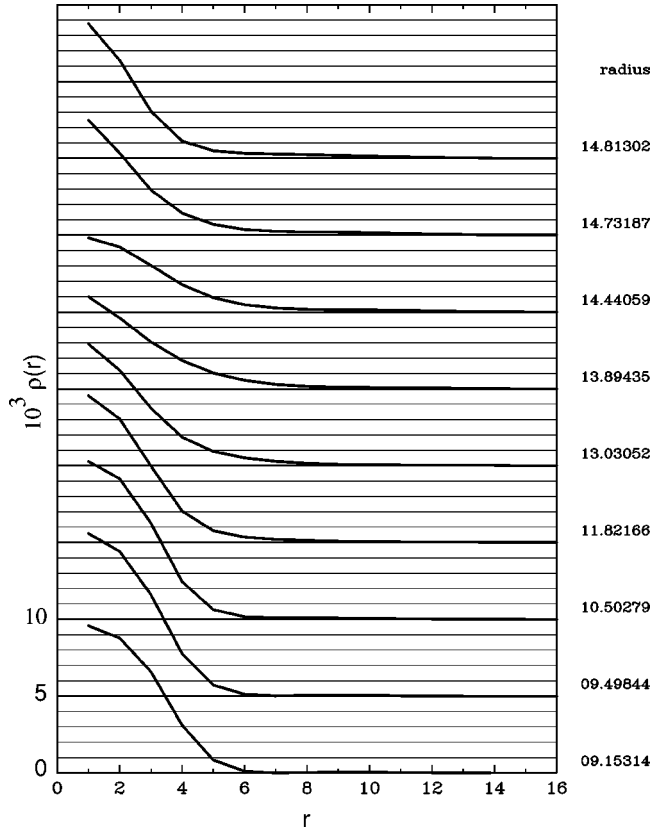

FIG. 6. Cycle on the main breathing line, $N=64$, $E=-0.9\times10^{-3}$, and $\tau=259.9276$.

other mode of oscillation of the system. But the order of magnitude of this ratio is not the same: real resonances tend to have ratios of order 1 false resonances tend to have ratios of order N. The distinction should become more and more apparent as N increases, although there will always be a middle region of ratios, appreciably larger than 1, but appreciably smaller than N, where most of the resonances will be partly real and partly false. In fact, for the comparatively small dimensions with which we have worked so far, this is essentially what happens. The width of the resonances also behaves differently in the two cases. For a real resonance, the width should remain stable as N increases. For a false one the width, usually small, can be highly variable.

Some of these conclusions can be checked by looking at the nuclear density as a function of space and time. We show the latter in Figs. 3–6 for four cycles along the main breathing line (or bottom envelope). All four of them exhibit simple breathing motion, although it is plain that those at higher energies contain some admixtures of low harmonics. By contrast we show in Fig. 7 the density for what appears to be a false resonance: we show two cycles at the same high energy ($E=0$), on opposite sides of the first, very thin, $N=32$ resonance. The curves show obviously that the breathing mode is mixed very strongly with harmonic 7 and, moreover, that the components of this seventh harmonic in the two cycles are out of phase by 180°, everything else being the same — a typical resonancelike feature. We show a more complicated case in Fig. 8. Again we have two cycles at $E=0$, this time for $N=64$, on opposite sides of a more ''substantial'' resonance — i.e., wider and probably partially real. One can distinguish a good amount of third harmonic and of eighth harmonic. Once again the two components of the eighth harmonic are out of phase with each other. We guess,

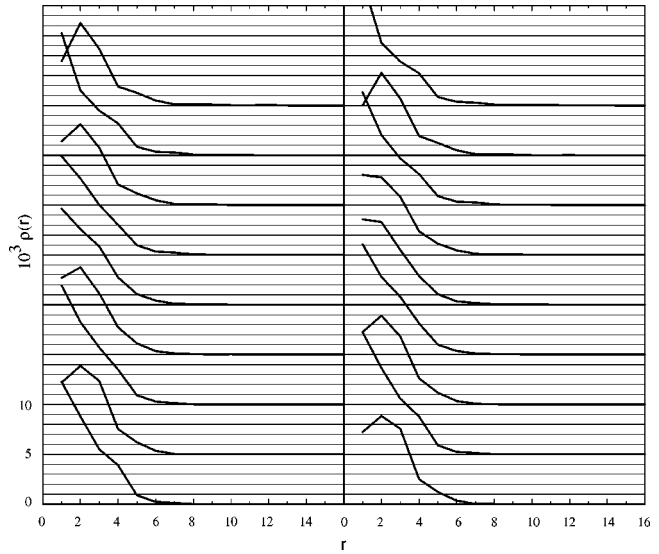

FIG. 7. Two cycles on both sides of the first, very thin, $N=32$ resonance. $E=0$ for both, $\tau=218.6627$ on the left, $\tau=218.6648$ on the right. The radii have been omitted for lack of space.

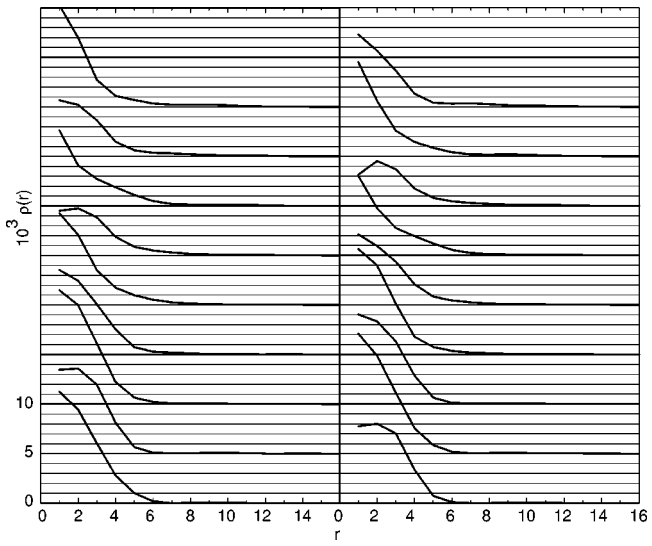

FIG. 8. Two cycles on both sides of a not so thin, $N=64$ resonance. $E=0$ for both, $\tau=255.9164$ on the left, $\tau=256.1675$ on the right.

without proof, that the third harmonic is probably real and the eighth false.

VIII. OUTLOOK

We embarked on this work in order to improve by an order of magnitude the accuracy of the calculations. We succeeded, but we are now facing new problems.

Our goal has not changed. It is to provide accurate, dependable calculations, in the mean-field approximation, with full nonlinearity, of actual physical nuclei. We want to include many shells, we want to include deformation, and therefore we need to work in two dimensions at least. The point of this paper was to develop a new method and to test it on the simplest of all closed-shell nuclei, helium. This is now done. We could generate more results for helium by going to higher N — for instance, $N=128$. This would be perfectly possible, but it is pointless, given that helium itself is not that interesting.

We intend to go on and apply this method to more interesting nuclei, beginning with the breathing modes of ^{16}O and ^{40}Ca. However, we must also attend to the problem of resonances which has surfaced as the result of this work. It is imperative that we be able to distinguish between the real and false resonances. The false resonances just do not belong in a reasonable physical theory. Actually, the more narrow real resonances do not belong either, since they should be eliminated by quantization, as we said earlier. Thus we must have a way to retain only the reasonably wide real resonances.

We have been working on this problem for quite some time now, and we think that we have a solution. Without compromising any of the accuracy attained by the method of the present paper, we think that we can Fourier transform from the time variable to the frequency variable and then drop the high frequencies from the equations. In other words, instead of a time mesh, we would use a frequency cutoff. The false resonances would be gone, since they are an artifact of the finite time step. And the narrow real resonances would be mostly gone also, since they usually involve mixing with higher frequencies than do the wide ones. We intend to publish the details once we have accumulated a sufficient collection of results.

ACKNOWLEDGMENTS

M.B. thanks Ben Mottelson for a stimulating conversation. Partial support for this work was received from the following agencies: the U.S. Department of Energy (DOE) under Grant Nos. DE-FG02-97ER41044 and DE-AC05-96OR22464 with Oak Ridge National Laboratory, managed by Lockheed Martin Energy Research Corp.; and the DOE under cooperative agreement No. DE-FC02-94ER40818 with the Massachusetts Institute of Technology. J.S.W. thanks the North Carolina Supercomputing Center (NCSC) for support.

[1] J.-S. Wu, K.C. Wong, M.R. Strayer, and M. Baranger, Phys. Rev. C **56**, 857 (1997).
[2] J.-S. Wu, M.R. Strayer, and M. Baranger, Phys. Rev. C **60**, 044302 (1999).
[3] M. Baranger and M. Véneroni, Ann. Phys. (N.Y.) **114**, 123 (1978).
[4] G. Bertsch, P.F. Bortignon, and R.A. Broglia, Rev. Mod. Phys. **55**, 287 (1983).
[5] F. Iachello and I. Talmi, Rev. Mod. Phys. **59**, 339 (1987).
[6] K.T.R. Davies, K. Devi, S.E. Koonin, and M.R. Strayer, in *Treatise on Heavy-Ion Science*, edited by D.A. Bromley (Plenum, New York, 1985), Vol. 3, p. 1.
[7] J.W. Negele, Rev. Mod. Phys. **54**, 913 (1982).
[8] H. Flocard, S.E. Koonin, and M.S. Weiss, Phys. Rev. C **17**, 1682 (1978).
[9] I. Zahed and M. Baranger, Phys. Rev. C **29**, 1010 (1984).
[10] M. Baranger and K.T.R. Davies, Ann. Phys. (N.Y.) **177**, 330 (1987); M.A.M. de Aguiar, C.P. Malta, K.T.R. Davies, and M. Baranger, *ibid.* **180**, 167 (1987); M. Baranger, K.T.R. Davies, and J.H. Mahoney, *ibid.* **186**, 95 (1988); K.T.R. Davies, T.E. Huston, and M. Baranger, Chaos **2**, 215 (1992).